Proceedings of the IASS 2024 Symposium
Redefining the Art of Structural Design
August 26-30, 2024, Zurich, Switzerland
Philippe Block, Giulia Boller, Catherine DeWolf,
Jacqueline Pauli, Walter Kaufmann (eds.)

Determination of stiffness requirements and design of appropriate small-scale stiffener layouts for robust lightweight metal shells

Alex SEITER*, Martin TRAUTZ*

* Chair of Structures and Structural Design (Trako), RWTH Aachen University
Schinkelstr, 1, 52062 Aachen, Germany
seiter@trako.arch.rwth-aachen.de

Abstract

Stiffening by forming beads in metal construction is an established lightweight construction strategy for making thin sheets resistant against bending and compressive stresses. Applied to construction and architecture, this is tantamount to activating thin sheets to transform them into surface-active load-bearing structures. The authors have already proposed systems that can be used in large-scale structures and have proven their efficiency with demonstrators (see Fig.1). The systems consist of either one or two layers of sheet metal (see Fig.2). In this article, approaches to test the applicability of stiffened sheet metal systems for large-scale structures are presented and applied to a case study problem. The motivation for the development of simplified approaches is the occurrence of a multi-scale problem that arises with explicit geometry modeling of small-scale stiffeners in large structures and pushes numerical simulations to their limits. The approaches are based on the assumption that stability failure forms the limits of the load-bearing capacity of these structures. In addition to the approach shown, the authors also pursue other, in principle similar approaches, so that the approach shown is representative.

Keywords: conceptual design, morphology, form finding, optimization, sheet metal shells, metal spatial structures, stability,

1. Introduction

The high level of primary energy required for sheet metal production is offset by the potential for material-efficient lightweight structures and the circular economy due to a high level of durability, disassembly and reusability. Such highly efficient structures are achieved by applying principles of structural morphology on global and local scale. While local stiffening can significantly increase the load-bearing capacity of thin sheet metal, on a global scale, efficient shell shapes can be determined using well-known form finding processes [1][2][3]. The combination of stretch forming (SF) and incremental sheet forming (ISF) allows the production of such optimized structures from basic metallic semi-finished products. The stiffeners are created by forming and not by adding material. This is in line with the principles of lightweight design. The authors have so far realized demonstrators in single-layer and double-layer construction [4] [5] [6].

Figure 1: Air Foil Pavilion - Demonstrator made out of two layers of 0.8mm stainless steel sheets

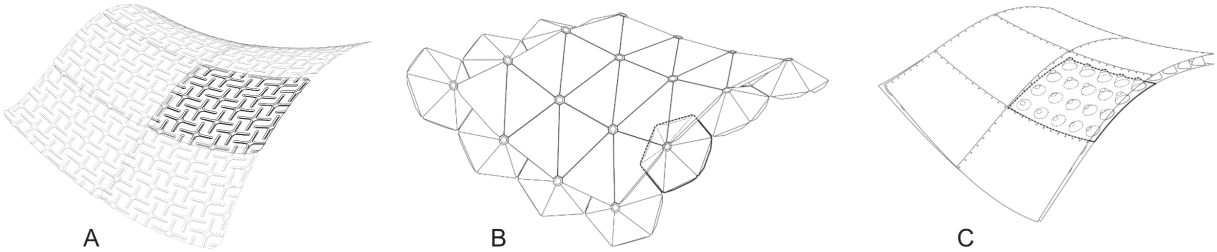

Figure 2: Principles of stiffening A) single layer B) double layer with tesselated curvature C) double layer with continuous curvature (as used for Air Foil Pavilion)

Determining the necessary stiffness of the structure is crucial, especially when designing for sufficient safety to prevent stability failure [3][7]. The size ratio of the overall structure to the local stiffeners leads to a multi-scale problem in numerical models. Explicit modeling of the geometry is not appropriate. The loss of the governing load case as an additional challenge for lightweight structures dramatically increases computation time. To determine the required stiffness of arbitrary structures, an iterative optimization process (IPSP) has been developed, where only the mid-surface of the structure needs to be modeled. During the stability analysis, IPSP iteratively increases the stiffness only in relevant surface domains until the required overall stiffness is achieved. All relevant load cases can be considered. In parallel, a method has been developed for determining the explicit stiffnesses of different stiffener layouts, specifically on small sections with explicit geometry modeling (ESDP). By comparing the IPSP and ESDP results, it is possible to determine which layouts provide sufficient overall stability for the structure. It should be noted that only the IPSP is dependent on the structure under analysis, while the ESDP needs to be performed only once for each stiffener layout.

2. Background

Improving the stability and vibration behavior of sheet metal structures is an optimization problem. There are various optimization approaches to the solution. The most common application is topology optimization, with the SIMP method (Solid Isotropic Material with Penalization) as the mathematical basis. This method goes back to Bendsoe and Kikuchi [8] [9] and Rozvany and Zhou [10]. An optimal material distribution can be determined within a system with defined loads, boundary conditions and also restrictions from production [11].

Simplified, this method determines for each point in the system whether material must be present or not. When the structure is discretized into finite elements, each element represents one of these points. In the SIMP method, the elements are referred to as isotropic solid microstructures. When material is needed they are filled, when no material is needed they are empty (cavities).This leads to a discrete density distribution within a system. A binary value is assigned for each element: $\rho(e) = 1$ where material is required and $\rho(e) = 0$ when material is removed [11]. Instead of assigning binary values, relative density distribution functions can be defined. By introducing a continuous relative density distribution function, the binary and one-sided nature of the problem is avoided. The relative density of the elements then varies between a minimum value ρ_{min} and the maximum value 1, which corresponds to porous elements according to the SIMP method. Since the relative material density can vary continuously, the modulus of elasticity can also vary continuously for each element. For each element e, the relationship between the relative material density factor ρ_e and the modulus of elasticity of the associated isotropic material model E_0 is calculated using the power law. The existing stress intensity of the elements is usually used as an optimization condition [11].

In contrast to the approaches found in the literature, the focus here is not on determining the position and size of stiffeners or infiltrations, i.e. discrete material concentration, but on a homogeneous stiffness distribution with the lowest possible maximum value. Although the thin sheet panels can be varied within a large structure, discrete variations in stiffness are not feasible in terms of design and are also not desirable. For the IPSP, optimization conditions and functions are therefore defined that differ from the classical method in order to determine the required stiffness distribution. These approaches are described in chapter 3.1.2. The conditions and functions are specially geared to the investigation of stability.

3. Methodology

The entire method can be divided into three main components, two of which function independently of each other. One of the two independent components is the IPSP. Here, the required stiffness of a structure is determined using boundary conditions. As this process is design-dependent, it must be run through for each initial geometry. The process is iterative and has a unique solution. The second independent component is the ESDP with which explicit stiffnesses of different panel systems are determined. This process is design-independent and only needs to be run once for each stiffener layout. The third component matches the results of the other two components and is therefore the last component in the entire method. This component can be used to assess whether a panel system or stiffening layout provides a structure with sufficient stability. Regarding to comparative analyses this approch allows the user get a better understanding of the structural behaviour of the global structure and its fast otimization ability, as well as a better understanding of how different stiffener layouts perform. Additionally the process is overall very robust, time saving, controllable, customizable and monito

3.1. Iterative Partial Stiffening Process (IPSP)

The objective function of the iterative process is sufficient stability $(loadfactor\lambda > 1.0)$ of the structure under different boundary conditions. This should be achieved with the lowest possible stiffness and the highest possible homogenity of the stiffness distribution. The process is set up as a single-objective optimization and not as a multi-objective optimization. The function is:

$$P : min[\lambda_i(X_i, Y_i)] > 1.0 \tag{1}$$

X_i and Y_i are represent different conditions and functions to increase the stiffness.

3.1.1. Procedure

First there is the definition of an initial geometry as a continouus surface, by form finding methods as dynamic relaxation or classic design strategies. The surface gets subdivided, e.g. according to the layout of the structual components. Note that this subdivision has no affection to the mesh densitiy for calculation. With a higher amount of subdivision the finer the resulting stiffness distribution gets. After subdivision constraints (loads, supports) can be defined. Next, the load factor λ_0 and the associated buckling shape $w(\lambda_0)$ are determined based on a buckling analysis. The buckling shape is then applied to the undeformed structure as a preload. This results in an internal bending moment and bending energy is introduced into the system. The stiffness of each subsurface can be increased after comparison of the values of each partial surface with the stiffness increase conditions. After adjusting the stiffness matrix, the process is repeated until the optimization goal is achieved. The flowchart in Fig. 3 shows the single steps.

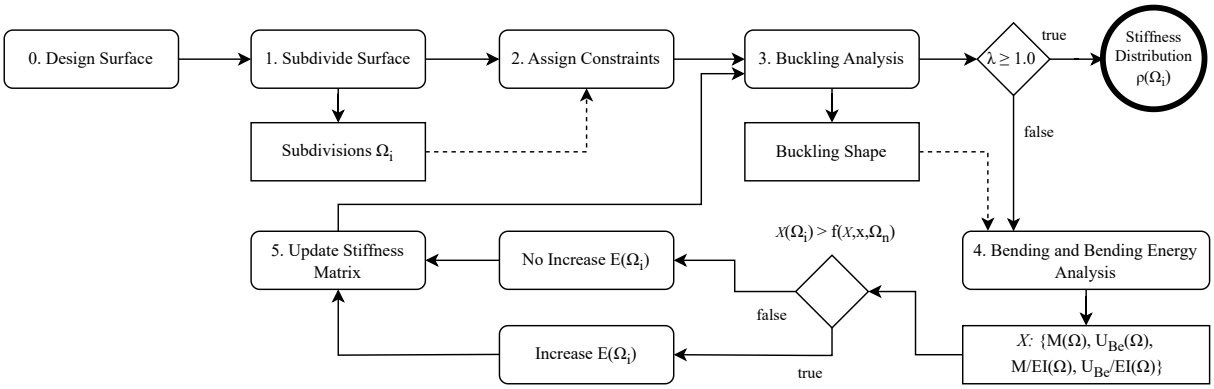

Figure 3: Procedure of IPSP

3.1.2. Conditions and Functions for Stiffness Increase

The authors have already investigated four different conditions for increasing stiffness and four different density functions.

Conditions X_i are :

$$\begin{aligned} \textit{Bending Moment: } & \bar{M}(\Omega_n) \\ \textit{Curvature: } & \kappa(\Omega_n) = \frac{\bar{M}(\Omega_n)}{EI(\Omega_n)} \\ \textit{Bending Energy: } & U_{Be}(\Omega_n) = \int_A \frac{\bar{M}^2(\Omega_n)}{2EI(\Omega_n)} \mathrm{d}A(x) \\ \textit{Bending Energy over Bending Stiffnes: } & \frac{U_{Be}(\Omega_n)}{EI(\Omega_n)} = \int_A \frac{\bar{M}^2(\Omega_n)}{2EI^2(\Omega_n)} \mathrm{d}A(x) = \int_A \frac{\kappa^2(\Omega_n)}{2} \mathrm{d}A(x) \end{aligned} \tag{2}$$

Density functions Y_i are:

$$\begin{aligned} &\textit{Absolute: Increase when } \kappa(\Omega_n) > 0.9\, max[\kappa(\Omega_n)] \;\; by factor \;\; \Delta\rho(\Omega_n) = 1.1 \\ &\textit{Linear: } \rho(\Omega_n) = 1 + 0.1\, x \frac{1}{max[\kappa(\Omega_n)]} \\ &\textit{Sinusoidal: } \rho(\Omega_n) = 1 + 0.1\, sin\left(x \frac{\pi}{2\, max[\kappa(\Omega_n)]}\right) \\ &\textit{Sinusoidal}^2\textit{: } \rho(\Omega_n) = 1 + 0.1\, sin^2\left(x \frac{\pi}{2\, max[\kappa(\Omega_n)]}\right) \end{aligned} \tag{3}$$

Based on previous results, the most promising combination is applied in this article. This includes the curvature based approach with the sinusoidal density function.

By consideration of the local curvature, the moment load has an influence on the optimization, but the local stiffness is also taken into account at the same time. This means that the change in the stiffness matrix in the previous iteration steps not only determines the buckling shape but also directly when determining the optimization variables. In particular, the approach implies that already optimized areas are weighted at a reduced level despite high stresses. This leads to an homogenous distribution.

The sinusoidal density function is related to the sinusoidal buckling figure and the resulting sinusoidal moment load applied from this as a prefabrication. This approach offers the best homogeneity properties and the lowest maximum value.

3.2. Explicit Stiffness Determination Process (ESDP)

Using the ESDP, it is intended to estimate the difference in the bending stiffness of surfaces with stiffeners compared to unstiffened surfaces. For this purpose, buckling values of different basic geometries are determined using uniform boundary stresses. Once for surfaces without stiffeners and once for the same surfaces with a specific stiffener layout. The factor of the buckling resistance of the same basic geometries is equivalent to the factor of the bending stiffness, because the correlation applies [12]:

$$k = \frac{\sigma_{crit}}{\sigma_e} \;\; with sigma_e = reference stress \tag{4}$$

The following applies for plane systems:

$$\sigma_{crit} = k \cdot \frac{E\pi^2}{12(1-\mu^2)} \left(\frac{t}{b}\right)^2 \quad so \quad p_{crit} = k \cdot \frac{Et^3\pi^2}{12(1-\mu^2)b^2} = k \cdot \frac{EI}{c_1} \tag{5}$$

It can be written for any system:

$$p_{crit} = c_2 \cdot \frac{EI}{c_1} = c \cdot EI \tag{6}$$

By introducing the load factor:

$$\lambda \cdot p_0 = c \cdot EI \tag{7}$$

Equation (7) shows the proportionality of the bending stiffness and the buckling factor. For a locally stiffened surface, based on the same basic geometry, its assumed that the increase in buckling stiffness is caused by an increased bending stiffness EI. The geometric coefficient c_2 remains unchanged.

3.2.1. Definition of the basic geometries

We examine square shells whose geometry is defined by the curvature of the four edges $(X0, X1, Y0, Y1)$. Each edge can assume a curvature k_i between the values -0.5 to 0.5 (see Fig. 4), with a step size of 0.1.

All combinations of these curvatures of non-congruent geometries are examined. Congruent geometries are exemplary:

$kX0 = kX1 = 0.5, kY0 = kY1 = -0.5$ and $kX0 = kX1 = -0.5, kY0 = kY1 = 0.5$.

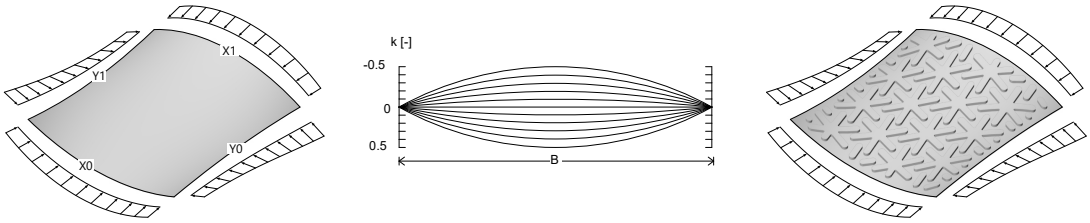

Figure 4: Scheme of basic geometry for investigation by ESDP

There are basically four cases for combinatorics. All edges positive M_1, three edges positive M_2, two opposite edges positive M_3 and two neighboring edges positive M_4. There are 480 possible combinations obtained by subsequent linear transformation and Gauss's summation formula.

The buckling value is determined for all 480 basic geometries using a uniform boundary stress. These buckling values are later compared with the buckling values of double-layer stiffened systems. In this way, the degree of system optimization in terms of stability can be determined for the different stiffening layouts.

4. Application based on a case study

In this paper, we consider a doubly curved shell as the initial geometry to calculate the required stiffness distribution considering two different load cases. The initial shell geometry is the result of the form finding process assuming a certain bending stiffness of the surface as shown in Fig. 5. The perimeter in the floor plan and the position of the supports were implemented as constraints. The form was determined by a uniform vertical load representing the dead weight of the structure. There are the two load cases applied, the distribtued load which served to find the shell form (LC1) as well as a concentrated area load perpendicular to the geometry (LC2).

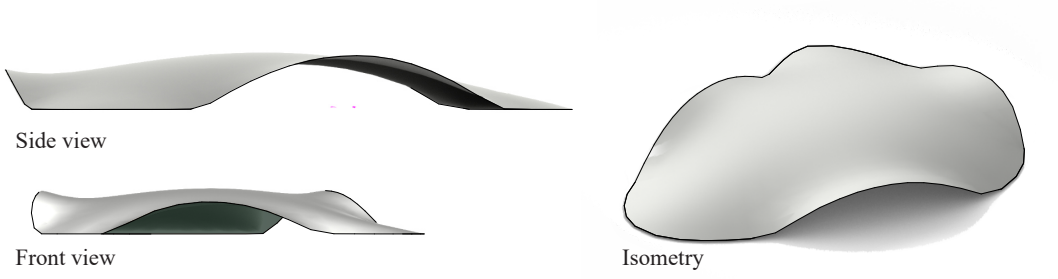

Figure 5: Geometry of shell geometry determined by form finding

4.1. IPSP Results for both Load Cases

The *initial surface* Ω_0 is getting subdivided into 421 *subsurfaces* Ω_n. Each of these subsurface represanting a structural component e.g. a sheet metal panel. For the structural component a single stiffness value is defined. This values getting calculated later on in section 4.2. Therefore during the iterative process the stiffness of subsurfaces is uniform.

Load cases are set up that the initial *buckling factor* λ is approx. 0.1 (10% of the apllied load). The solution counts as converged when λ reaches 1.0. This means the convergesd solution represents the stiffness distribution of the structure required to carry the applied load. The two load cases get calculated seperatly to stress out the difference between the uniformly distributed load (LC1) and the concentrated load (LC2). The results of the two calculations get matched for having the final solution, able to carry both loads. The procedure would allow to calculate both load cases simultaniously, but for clarity, they are considered separately here.

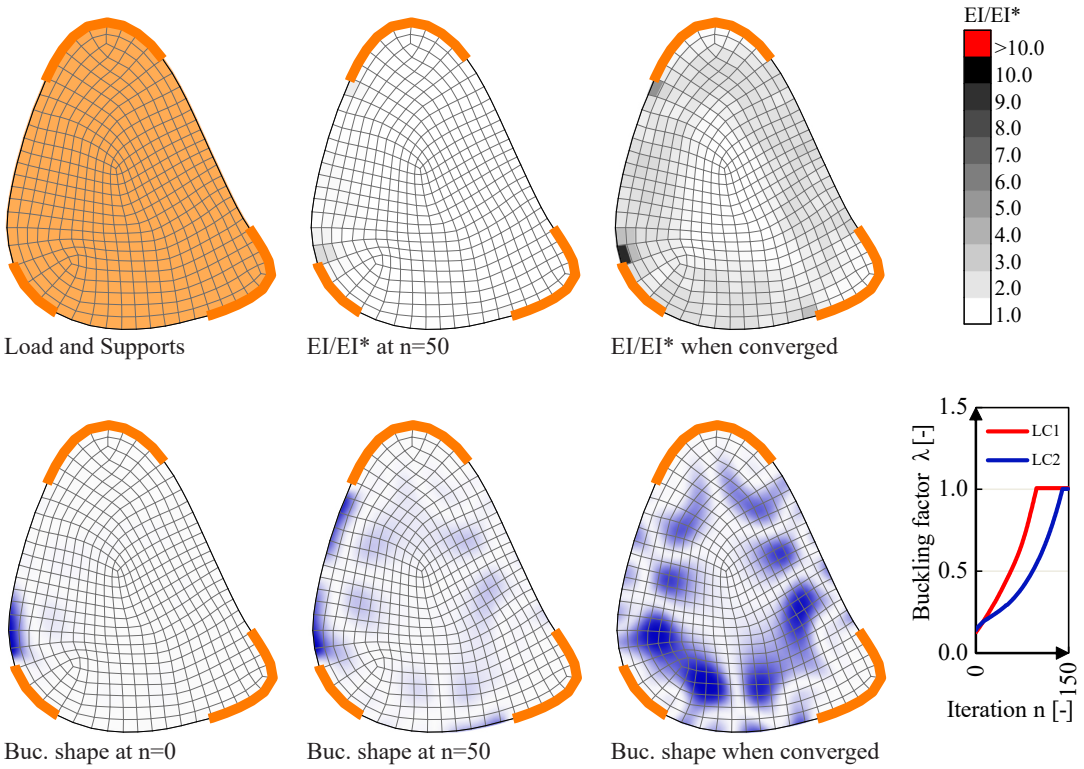

Figure 6: IPSP Results for LC1

In load case 1 (uniformly distributed and constant surface load), the structure buckles quite locally at the transition from the free edge to the support (see Fig. 6). The increase in stiffness is also concentrated at the same point in the first iterations. After 50 iterations, the strongly localized buckling has spread not only to the entire free edge but also over the entire shell structure, exept the apex. This is followed by an increase in the stiffness of the individual subsurfaces. The solution converged after approx. 100 iterations shows a rather global buckling pattern. Three main buckles occur between the apex and the support. The initial local buckling occurs in a significantly weakened form. The final stiffness distribution is largely homogeneous with the exception of two subsurfaces in the area of the initial buckling. In load case 2 (concentrated load in the area of a free edge), the buckling is completely locally near the support (see Fig. 7). After 50 iterations, the buckling expands along the entire free edge at the load. Until the

last iteration, this area continues to expand without spreading to the other side of the shell structure. Approx. 150 iterations are necessary for the solution to converge. In contrast to load case 1, the stiffness distribution is less homogeneous with higher maximum stiffnesses. This is to be expected due to the concentrated load application.

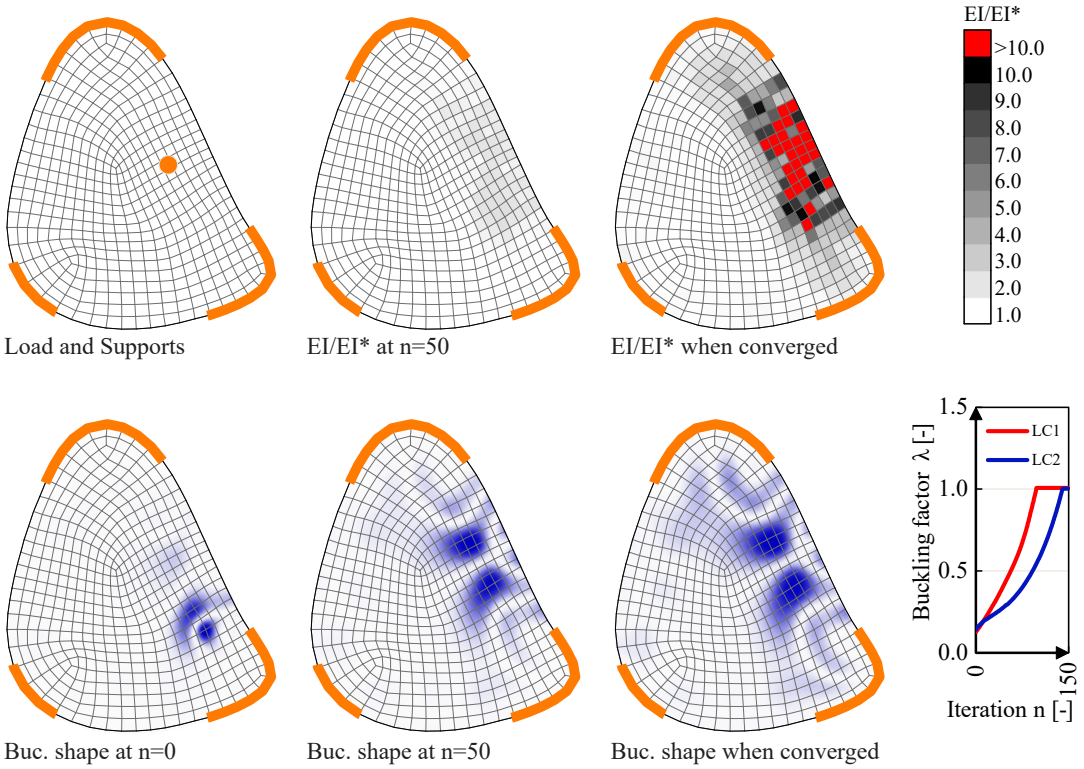

Figure 7: IPSP Results for LC2

The result of the superposition of the two load cases is shown in Fig. 8. Each partial area is assigned the maximum of the required stiffness from the two load cases. In addition to superposition, the authors also examined a continuous calculation. In this case, the stiffness distribution from the previous load case is used as the starting point. The results are basically the same, but there are deviations which show that the IPSP solutions are local optima.

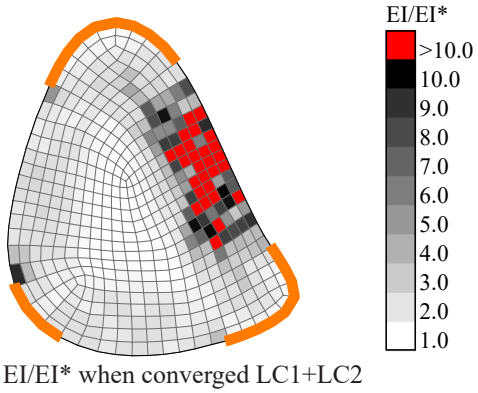

Figure 8: Superposition of IPSP results of LC1 and LC2

4.2. ESDP of the considered stiffening system

A two-layer system with star-shaped stiffening geometries is being investigated. The buckling values were determined for all 480 basic geometries defined in chapter 3.2. In each case for the single-layer system without stiffeners and the pattern described above. Figure 9 shows the results with the stiffness factor *EI/EI** on the y-axis. The different basic geometries are represented by the x-axis, sorted according to the four categories M_1-M_4 in chapter 3.2.

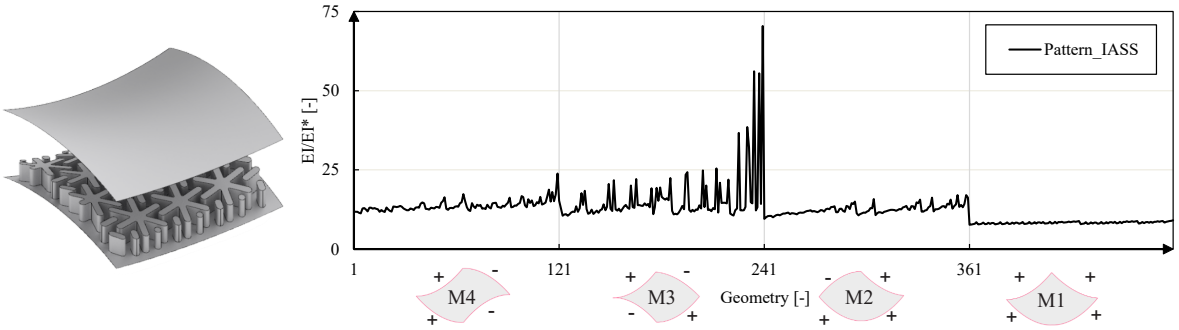

Figure 9: ESDP results of 480 geometries with starform pattern

The surfaces of category M_1 all have a positive Gaussian curvature. In this category, the unstiffened surfaces have by far the highest buckling values, up to 80 times higher than a flat surface. Buckling only occurs very locally in the area of load application. Therefore, the stiffening has less influence on the buckling values, the factor *EI/EI** is sometimes just above 7. (Fig. 9). In the categories M_2-M_4, the stiffeners have a significantly greater influence, the minimum values of the *EI/EI** factors here are approx. 12. Category M_3 shows the highest variation. Here, a wide range of buckling occurs in the unstiffened surfaces: Very locally limited single buckles, diagonal and central global single buckles and checkerboard-like buckling.

4.3. Matching Results

To match the results of the IPSP and the ESDP, the partial surfaces defined in the IPSP are correlated to a basic geometry of the ESDP. The correlation is made by comparing the four edge curvatures. If the stiffness factor determined using the ESDP is higher for all partial surfaces than the minimum value determined using the IPSP, the stiffening pattern is suitable for providing the structure with sufficient overall stability. This is the case in the shown case study.

5. Conclusion

The method presented can be used to efficiently test sheet metal construction systems with individual stiffening layouts for their suitability for use as load-bearing structures for large-scale structures of arbitrary shape. The ESDP must be further refined. In the next step, geometry properties other than the edge curvatures must be defined in order to assign a result value from the limited set of analyzed geometries to an arbitrarily shaped subsurface. The current approach is only suitable for defining a lower limit value. An approach that takes into account the bending energy released during buckling and an approach based on the Gaussian curvature intensity are being pursued further. The IPSP, on the other hand, proves to be a straightforward process with no limitations. Even detached from the context of lightweight metal construction, it can generally be used to determine minimum system stiffnesses regardless of the construction method or materiality.

Acknowledgments

All demonstrators and construction systems were developed and realized in cooperation with the Institute of Metal Forming (ibf) at RWTH Aachen University. Research projects for realising the demonstrators were funded by the AiF and ZukunfBau.

References

[1] J. Wiedemann, *Leichtbau 1: Elemente*, 2., neubearb. Aufl. Berlin Heidelberg: Springer, 1996.

[2] J. Wiedemann, *Leichtbau 2: Konstruktion*, 2., neubearb. Aufl. Berlin Heidelberg: Springer, 1996.

[3] B. Klein, *Leichtbau-Konstruktion*. Wiesbaden: Springer Fachmedien Wiesbaden, 2013.

[4] A. J. Seiter, T. C. Pofahl, M. Trautz, L.-M. Reitmaier, D. Bailly, and G. Hirt, "Sheet Metal Shells," in *14. Baustatik Baupraxis.*, ser. Baustatik Baupraxis, vol. 14, Institut für Baustatik und Baudynamik, Universität Stuttgart, 2020, pp. 439–446.

[5] T. C. Pofahl, A. J. Seiter, M. Trautz, L.-M. Reitmaier, D. Bailly, and G. Hirt, "Form Finding of a Sheet Metal Shell by Generative Design and Pareto Optimization," in *Advances in Architectural Geometry*, Berlin ; Boston: De Gruyter, 2023, pp. 269–382.

[6] M. Trautz, T. C. Pofahl, A. J. Seiter, G. Hirt, L.-M. Reitmaier, and D. Bailly, "Leichtbaukonstruktionen aus Feinblech," *Stahlbau*, vol. 91, no. 6, pp. 375–384, 2022.

[7] A. Öchsner, *Leichtbaukonzepte anhand einfacher Strukturelemente: Neuer didaktischer Ansatz mit zahlreichen Übungsaufgaben*. Berlin, Heidelberg: Springer, 2019.

[8] M. P. Bendsøe and N. Kikuchi, "Generating optimal topologies in structural design using a homogenization method," *Computer Methods in Applied Mechanics and Engineering*, vol. 71, no. 2, pp. 197–224, Nov. 1988.

[9] M. Bendsoe, "Optimization of structural topology, shape, and material," 1995.

[10] G. I. N. Rozvany, Ed., *Shape and Layout Optimization of Structural Systems and Optimality Criteria Methods*. Vienna: Springer, 1992.

[11] SolidWorks. "Simp method for topology optimization." (2019), [Online]. Available: `https://help.solidworks.com/2019/english/solidworks/cworks/c_simp_method_topology.html` (visited on 03/15/2024).

[12] C. Petersen, *Statik und Stabilität der Baukonstruktionen: Elasto- und plasto-statische Berechnungsverfahren druckbeanspruchter Tragwerke: Nachweisformen gegen Knicken, Kippen, Beulen*. Wiesbaden: Vieweg+Teubner Verlag, 1982.